NASA Technical Paper 3224

July 1992

An Analysis of Combustion Studies in Shock Expansion Tunnels and Reflected Shock Tunnels

Casimir J. Jachimowski

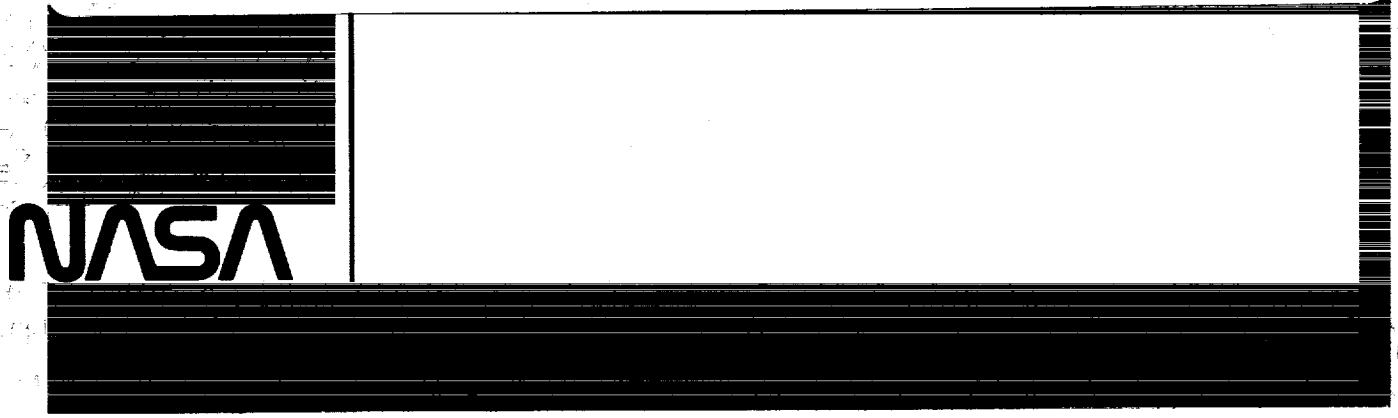

NASA Technical Paper 3224

1992

An Analysis of Combustion Studies in Shock Expansion Tunnels and Reflected Shock Tunnels

Casimir J. Jachimowski
Langley Research Center
Hampton, Virginia

NASA
National Aeronautics and Space Administration
Office of Management
Scientific and Technical Information Program

Abstract

The effect of initial nonequilibrium dissociated air constituents on the combustion of hydrogen in high-speed flows for a simulated Mach 17 flight condition was investigated by analyzing the results of comparative combustion experiments performed in a reflected shock tunnel test gas and in a shock expansion tunnel test gas. The results were analyzed and interpreted with a one-dimensional quasi-three-stream combustor code that includes finite rate combustion chemistry. The results of this study indicate that the combustion process is kinetically controlled in the experiments in both tunnels and that the presence of the nonequilibrium partially dissociated oxygen in the reflected shock tunnel enhances the combustion. Methods of compensating for the effect of dissociated oxygen are discussed.

Introduction

Currently, reflected shock tunnels and shock expansion tunnels are the only facilities that can generate high enthalpy conditions for simulation of scramjet combustion at flight Mach numbers greater than 12 (refs. 1 and 2). Even though each facility can simulate the enthalpies and combustor inlet Mach numbers representative of high flight Mach number conditions, the composition of the test gas or simulated air produced is significantly different in each facility. The reflected shock tunnel test gas contains significant amounts of atomic oxygen and nitric oxide because the test gas is brought to a stagnant condition prior to expansion to the desired high-energy flow conditions. Chemical kinetic effects prevent the recombination of significant amounts of the atomic oxygen and the reduction of nitric oxide to nitrogen and oxygen. In the shock expansion tunnel, the test gas is accelerated to the test condition by an unsteady expansion and is never brought to a stagnant condition. The highly dissociated test gas produced in a reflected shock tunnel is of special concern when used for combustion tests, which must be interpreted in terms of combustion in real air.

The presence of atomic oxygen in the test gas can affect combustion tests in several ways. Atomic oxygen reacts very rapidly with molecular hydrogen. If sufficient amounts of the atomic oxygen are present in the test gas, the test gas can be expected to be more reactive than real air. Also, the presence of atomic oxygen will increase the heat release by adding the heat of formation to the fuel heat content. In addition, under certain conditions the increased rate of hydrogen reaction in the presence of atomic oxygen can affect mixing (ref. 2).

Recently, a series of comparative experiments were performed at essentially identical conditions in a shock expansion tunnel (the NASA HYPULSE tunnel located at General Applied Science Laboratories (GASL)) and in a reflected shock tunnel (the University of Queensland T4 tunnel) (ref. 2). The purpose of the experiments was to determine the effects of test gas composition on combustion in high-speed flows. Each facility simulated combustor inlet conditions for a Mach 17 flight condition. The experiments were carried out with identical combustors—a constant area, axisymmetric combustor with an overall length-to-diameter ratio of 24. The fuel was injected through a singular annular slot at Mach 1.9 at an angle of 15° from the combustor axis.

The purpose of this study was to analyze and interpret the results obtained from the comparative experiments by using a one-dimensional quasi-three-stream combustor code that includes a finite rate chemistry description of the combustion process. An attempt was made to examine the role of chemical kinetics on the combustion of hydrogen in the two facilities, with special emphasis on the effect of dissociated air compared with nondissociated air.

Symbols

d	combustor internal diameter
H_s	stagnation enthalpy, MJ/kg
P	static pressure, kPa
P_o	average tare pressure from fuel-off tests, kPa
T	static temperature, K
T_s	stagnation temperature, K
U	velocity, m/s
x	axial location along combustor, cm
ϕ	fuel-to-total-oxygen equivalence ratio

Results of Comparative Experiments

The fuel-to-oxygen equivalence ratio was 3 in all the comparative experiments. The test conditions that were selected for the comparative experiments are listed in table I, where the test gas composition (air) is given as mole fraction. The results of the comparative experiments (shock expansion tunnel air and reflected shock tunnel air a) are given in figures 1 and 2. The results are expressed in terms of measured static pressure along the combustor normalized by the facility tare pressure P_o. The tare pressure is the average pressure in the combustor during fuel-off tests. The result shown in figure 1 is a comparison of the measured pressure distributions

Table I. Test Flow Conditions and Test Gas Composition (Mole Fraction)

	Shock expansion tunnel test gas	Reflected shock tunnel test gas		
		a	*b*	*c*
H_s, MJ/kg	15.3	15.7	15.7	15.7
T_s, K	8355	7880	8350	8180
T, K	2088	2065	2120	2037
P, kPa	16.5	15.3	15.1	15.1
P_o, kPa	24.8	14.7	14.7	14.7
U, m/s	5078	4710	4910	4819
O_2	0.2038	0.0898	0.0053	0.0274
N_2	0.7755	0.6956	0.8838	0.8070
O	0.0014	0.1614	0.0918	0.1318
NO	0.0099	0.0451	0.0103	0.0250
Ar	0.0094	0.0081	0.0088	0.0088
Mole percent total oxygen	21.0	21.1	5.9	11.4

for the hydrogen into nitrogen mixing runs in the two facilities. The good agreement between facilities indicates that flow interactions that occur when hydrogen is injected are similar in each facility. The result shown in figure 2 is a comparison of the measured pressure distributions for the hydrogen into air combustion tests. The results clearly demonstrate the pressure rise is greater in the reflected shock tunnel combustion test, presumably because of combustion enhancement by the dissociated test gas.

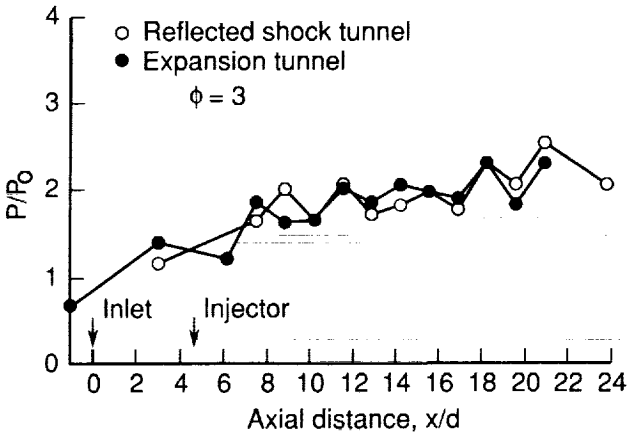

Figure 1. Static pressure distributions for hydrogen into nitrogen mixing test normalized by the average tare pressure for each facility.

Method of Data Analysis

Mathematical Combustor Model

The experimental results were analyzed with the combustor code SCRAM3, which was assembled pri-

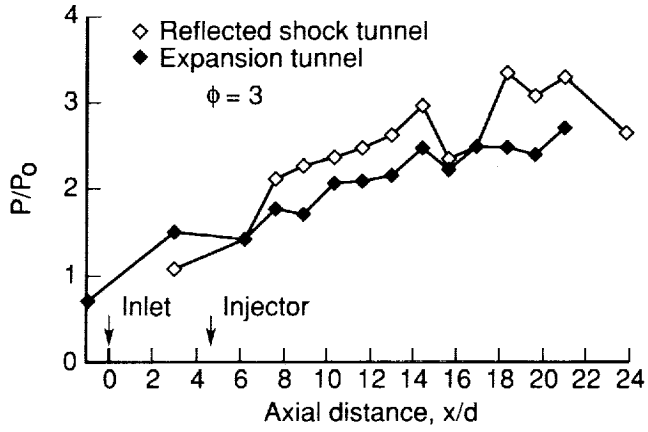

Figure 2. Combustion test static pressure distributions normalized by the average tare pressure for each facility.

marily to model high-speed reacting flows. The physical model in the code is based on a steady-state analysis of a reacting flow through an assigned area profile. The system of differential equations that describes the conservation of mass, momentum, energy, and finite rate chemistry is based largely on the codes described by Bittker and Scullin (ref. 3) and McLain and Rao (ref. 4). These codes treat the reacting flow as a homogeneous mixture in which all the reactants are initially premixed at a specified temperature and pressure. In SCRAM3, the unmixed fuel, unmixed air, and the reaction zone are treated separately. The SCRAM3 model is depicted in figure 3. Separate temperatures are assigned to the unmixed fuel, unmixed air, and the

ignition source. The ignition source represents a flame-holding region that provides free radicals and thermal energy for the ignition of the fuel and air. A mixing routine is included in the code, allowing the fuel and air to be mixed at a prescribed schedule along the combustor. The fuel and air initially mix with the ignition source constituents to form the reaction zone. The reaction zone volume increases down the combustor as more fuel and air are added. For this study, the mixed fuel and air are assumed to form a stoichiometric reaction zone until either the fuel (lean fuel-air combustor) or the air (rich fuel-air combustor) is fully mixed. The flow through the combustor is treated as a quasi-one-dimensional flow in which average system properties are used in the conservation equations. The differential equations that describe the finite rate chemistry use the species concentrations and temperatures in the reaction zone.

- Three-temperature model: fuel, air, reaction zone

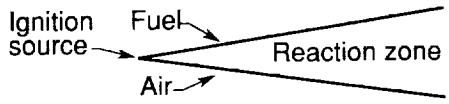

- Fuel and air are mixed in reaction zone through an assigned schedule, i.e., ϕ (Mixing) = 1
- Reaction zone chemistry described by detailed chemical kinetic reaction scheme
- Average system properties used in the mass, momentum, and energy equations in a one-dimensional steady-state flow through an assigned area profile

Figure 3. Elements of the SCRAM3 combustor code.

The chemical kinetic reaction mechanism and rate coefficients used to describe the combustion of hydrogen are listed in table II. The reactions and assigned rate coefficients are based largely on the chemical reaction scheme recommended by the NASP Rate Constant Committee (ref. 5). The rate coefficients used for reactions (2) and (10) were adjusted slightly to provide a reaction set that could reproduce ignition delay times and laminar flame speeds reported in the literature. The thermodynamic data for the chemical species recommended in the NASP report (ref. 5) were also used in the combustor code.

Data Analysis

To correctly simulate the combustion tests using the SCRAM3 combustor code, the effect of fuel injection on the flow through the combustor must be taken into account and a fuel-air mixing schedule must be specified. The results of the hydrogen into nitrogen mixing tests (fig. 1) clearly show that the fuel injection increases pressure along the combustor. The SCRAM3 code cannot model this interaction directly, but the effect can be taken into account by specifying a combustor area ratio that reproduces the observed pressure rise. To reproduce the pressure rise, the area ratio profile shown in figure 4 was required. This profile was determined by inputting the pressure distribution curve shown in figure 5 into the SCRAM3 code and allowing the code to generate the required area profile. The results given in figures 4 and 5 are plotted in terms of distance from the fuel injector.

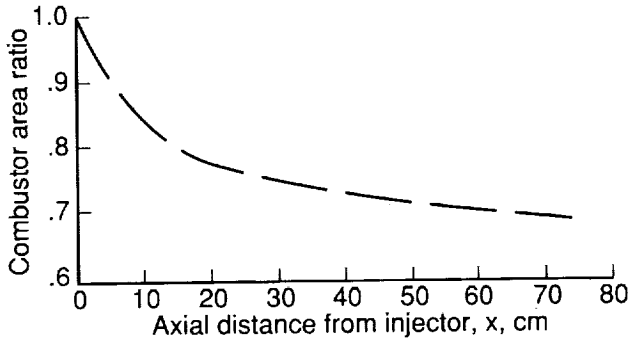

Figure 4. Combustor area ratio profile determined by SCRAM3.

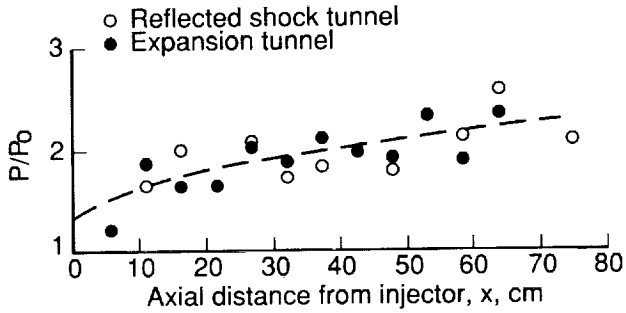

Figure 5. Pressure distribution used in SCRAM3 to determine the area ratio shown in figure 4.

To determine the mixing schedule for the fuel and test gas, the results of the HYPULSE expansion tunnel combustion test were used. The mixing distribution shown in figure 6, when used in the SCRAM3 code, produced the pressure profile shown in figure 7. The mixing fraction given in figure 6 is defined as the fraction of the total test gas that is mixed with and allowed to react with a stoichiometric amount of hydrogen. This method of determining the mixing schedule effectively assumes that the combustion

chemistry is accurately described by the reactions and rate coefficients listed in table II. Also, when matching the calculated pressure distribution with the observed pressure distribution no ignition source was used. Previous analytical studies (ref. 6) have shown that at air temperatures above 1500 K the presence of an ignition source did not significantly affect the subsequent reaction rates. To verify this conclusion, several runs were made in which up to 2 percent of the test gas was assumed to react to equilibrium with a stoichiometric amount of H_2 to form ignition source constituents. No significant effect was observed on the calculated results. Similar sensitivity studies were carried out with the University of Queensland T4 reflected shock tunnel test gas, and no affect was observed.

The area ratio profile and the mixing schedule shown in figures 4 and 6 were used in SCRAM3 for the analysis of all the reflected shock tunnel combustion experiments that are discussed in this report.

Table II. H_2-Air Reaction Mechanism[a]

Reaction[b]	A	B	E
(1) $H_2 + O_2 \rightarrow HO_2 + H$	7.00×10^{13}	0	56800
(2) $H + O_2 \rightarrow OH + O$	2.20×10^{14}	0	16800
(3) $O + H_2 \rightarrow OH + H$	5.06×10^{4}	2.67	6290
(4) $OH + H_2 \rightarrow H_2O + H$	2.16×10^{8}	1.51	3430
(5) $OH + OH \rightarrow H_2O + O$	1.50×10^{9}	1.14	0
(6) $H + OH + M \rightarrow H_2O + M$	8.62×10^{21}	−2.0	0
(7) $H + H + M \rightarrow H_2 + M$	7.30×10^{17}	−1.0	0
(8) $H + O + M \rightarrow OH + M$	2.60×10^{16}	−0.6	0
(9) $O + O + M \rightarrow O_2 + M$	1.10×10^{17}	−1.0	0
(10) $H + O_2 + M \rightarrow HO_2 + M$	2.30×10^{18}	−1.0	0
(11) $HO_2 + H \rightarrow OH + OH$	1.50×10^{14}	0	1000
(12) $HO_2 + O \rightarrow O_2 + OH$	2.00×10^{13}	0	0
(13) $HO_2 + OH \rightarrow H_2O + O_2$	2.00×10^{13}	0	0
(14) $HO_2 + HO_2 \rightarrow H_2O_2 + O_2$	2.00×10^{12}	0	0
(15) $H + H_2O_2 \rightarrow H_2 + HO_2$	1.70×10^{12}	0	3780
(16) $H + H_2O_2 \rightarrow OH + H_2O$	1.00×10^{13}	0	3580
(17) $O + H_2O_2 \rightarrow OH + HO_2$	2.80×10^{13}	0	6400
(18) $OH + H_2O_2 \rightarrow H_2O + HO_2$	7.00×10^{12}	0	1435
(19) $OH + OH + M \rightarrow H_2O_2 + M$	1.60×10^{22}	−2.0	0
(20) $N + N + M \rightarrow N_2 + M$	2.80×10^{17}	−0.8	0
(21) $N + O_2 \rightarrow NO + O$	6.40×10^{9}	1.0	6300
(22) $N + NO \rightarrow N_2 + O$	1.60×10^{13}	0	0
(23) $N + OH \rightarrow NO + H$	6.30×10^{11}	0.5	0
(24) $H + NO + M \rightarrow HNO + M$	5.40×10^{15}	0	−600
(25) $H + HNO \rightarrow NO + H_2$	4.80×10^{12}	0	0
(26) $O + HNO \rightarrow NO + OH$	5.00×10^{11}	0.5	0
(27) $OH + HNO \rightarrow NO + H_2O$	3.60×10^{13}	0	0
(28) $HO_2 + HNO \rightarrow NO + H_2O_2$	2.00×10^{12}	0	0
(29) $HO_2 + NO \rightarrow NO_2 + OH$	3.40×10^{12}	0	−260
(30) $HO_2 + NO \rightarrow HNO + O_2$	2.00×10^{11}	0	1000
(31) $H + NO_2 \rightarrow NO + OH$	3.50×10^{14}	0	1500
(32) $O + NO_2 \rightarrow NO + O_2$	1.00×10^{13}	0	600
(33) $M + NO_2 \rightarrow NO + O + M$	1.16×10^{16}	0	66000

[a]The rate coefficients are given in the form $k = AT^B e^{-E/RT}$; units are in seconds, moles, cubic centimeters, calories, and degrees Kelvin.

[b]Third body efficiencies for all termolecular reactions are 2.5 for M = H_2, 16.0 for M = H_2O, 4.0 for M = CO_2, and 1.0 for all other M.

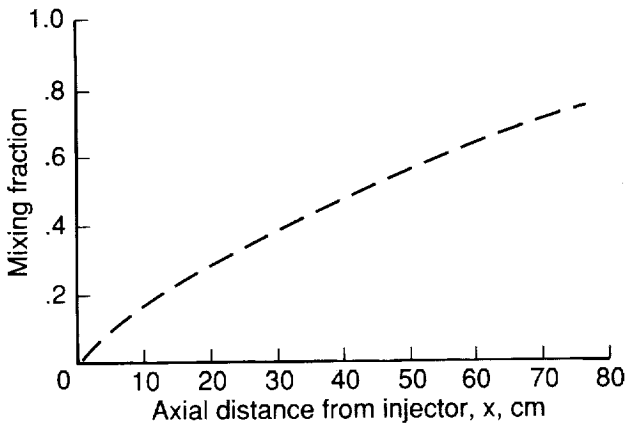

Figure 6. Mixing distribution for fuel and test gas determined from the HYPULSE expansion tunnel combustion data.

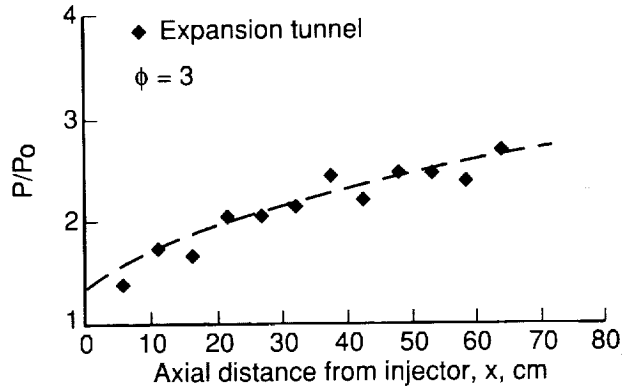

Figure 7. Pressure distribution used to determine the mixing distribution shown in figure 6.

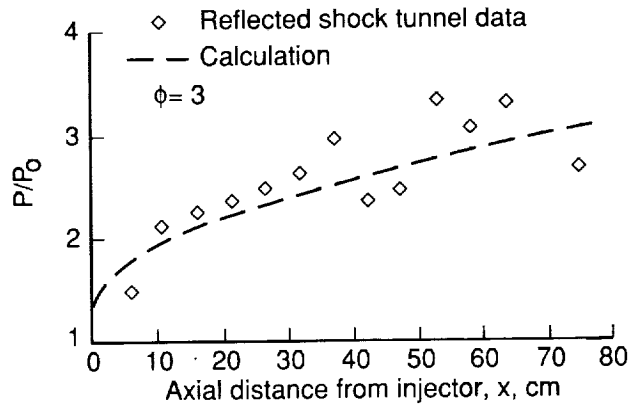

Figure 8. Calculated and experimental pressure distributions for reflected shock tunnel test gas *a*.

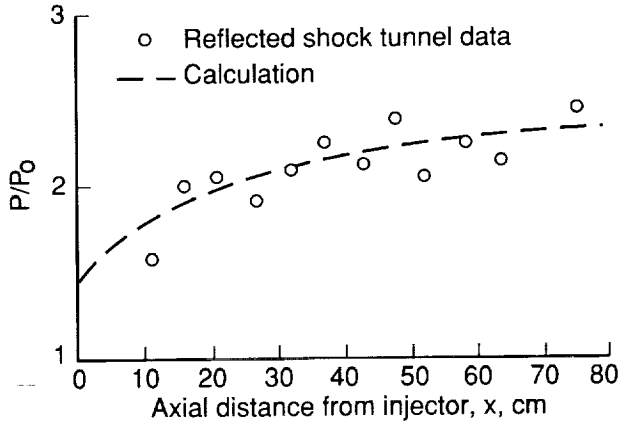

Figure 9. Calculated and experimental pressure distributions for reflected shock tunnel test gas *b*.

Results and Discussion

The calculated pressure distributions for the reflected shock tunnel experiment are shown in comparison with experimental data in figures 8 and 9. The experimental results in figure 8 are from the combustion test with tunnel test gas *a* (table I). The calculated pressure distribution is in very good agreement with the experimental data. The experimental results shown in figure 9 are from a combustion experiment with a test gas in which the oxygen content was reduced to 5.9 percent. The test flow conditions for this test gas mixture are listed in table I as reflected shock tunnel test gas *b*. This air mixture was an initial attempt to compensate for the effect of dissociated air and reproduce the expansion tunnel combustion results. Even though the measured pressure distribution for test gas *b* was not in good agreement with the HYPULSE expansion tunnel combustion results, the results of the SCRAM3 calculation are in very good agreement with the data, as shown in figure 9.

The ability of the SCRAM3 combustor code to predict pressure distributions that are in very good agreement with the experimental data suggests that the combustion model provides a reasonably accurate representation of the physical and chemical processes that control the combustion process in the expansion tunnel and reflected shock tunnel experiments examined in this study. Therefore, it seemed reasonable to use the code to investigate the role of chemical kinetics in the combustion experiments that were analyzed.

The importance of finite rate chemistry is shown in figure 10, in which the results of finite rate calculations are shown in comparison with the results of calculations in which equilibrium combustion chemistry is assumed and no reaction is assumed. These

comparisons indicate that the combustion process is controlled by the chemical kinetics in both the expansion tunnel experiments and the reflected shock tunnel experiments. The chemical kinetic effect is the result of the low combustion pressures and short residence times in the experiments. The difference in the pressure distributions in figure 10 is largely due to the slow rate of H_2O formation through reaction (6):

(6) $$H + OH + M \rightarrow H_2O + M$$

which is very sensitive to pressure.

Nitric oxide can enhance the combustion process by providing an alternate path for the formation of H_2O:

(24) $$H + NO + M \rightarrow HNO + M$$

(27) $$OH + HNO \rightarrow NO + H_2O$$

To be effective, the HNO radical must be produced in sufficient quantity to allow reaction (27) to occur. However, the rate of reaction (24) is also sensitive to pressure, and at the reflected shock tunnel combustion pressures the rate of HNO formation is negligible. The presence of nitric oxide in the reflected shock tunnel test gas does not enhance the combustion process. Removing the nitrogen and oxygen reactions (reactions (20)–(33)) did not affect the calculated results. The low combustion pressures are responsible for the lack of any effect. Calculations indicate that for the nitric oxide levels present in the reflected shock tunnel test gas, the nitric oxide reaction chemistry would become important at combustor pressures greater than 200 kPa.

To assess the effect of nonequilibrium dissociated oxygen on the combustion process, a parametric study was performed in which combustion in the reflected shock tunnel test gas was simulated using various assumptions about the test gas chemical composition and the atomic oxygen reaction chemistry. The conditions that were simulated are listed in table III. Simulation 1 represents combustion in reflected shock tunnel test gas *a* with the full chemical kinetic mechanism and the initial conditions listed in table I. Simulation 2 represents combustion in a real, nondissociated air test gas. By comparing the results from simulations 1 and 2, the net effect of the dissociated oxygen on combustion can be determined. Simulation 3 represents combustion in test gas *a* similar to simulation 1, but the reaction mechanism was altered to prevent any reaction of the test

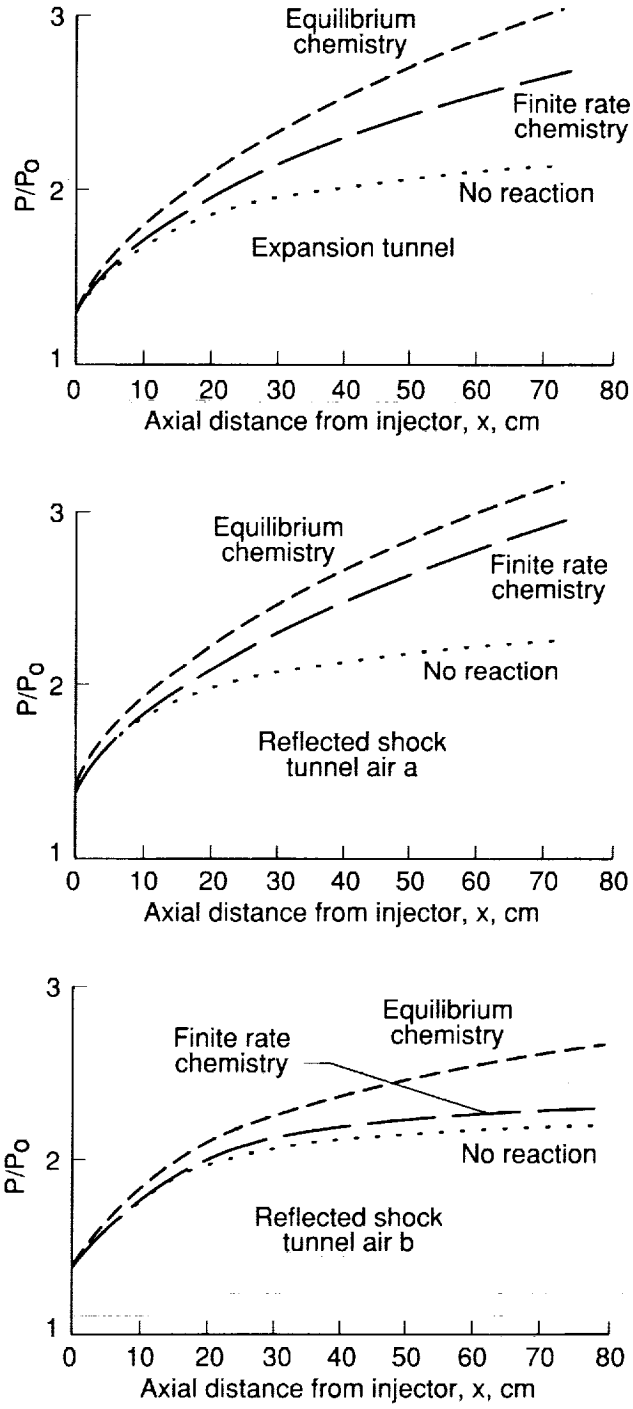

Figure 10. Effect of finite rate chemistry, equilibrium chemistry, and no reaction on the calculated pressure distribution.

gas oxygen atoms by treating them as inert species. In simulations 4 and 5, the test gas oxygen atoms were allowed only to recombine through reaction (9) to form molecular oxygen:

(9) $$O + O + M \rightarrow O_2 + M$$

Table III. Simulated Conditions

Simulation	Test gas	Reaction chemistry
1	*a*	No change
2	Nondissociated air	No change
3	*a*	Test gas oxygen atoms assumed inert
4	*a*	Inert test gas oxygen atoms allowed to recombine to form inert O_2
5	*a*	Inert test gas oxygen atoms allowed to recombine to form reactive O_2

However, in simulation 4 the molecular oxygen formed from the test gas atomic oxygen is treated as inert in the reaction mechanism so that the only contribution to the combustion process is the release of dissociation energy. In simulation 5, the molecular oxygen is treated as normal oxygen and allowed to react. By comparing the results from simulations 3, 4, and 5, the relative importance of reaction rate enhancement and dissociation energy heat release can be examined.

The results of the simulations are shown in figures 11 and 12. The pressure distribution along the combustor is plotted for each simulation. Also given in each figure is the total chemical energy released, in kJ/kg of reaction product, for each simulation. The results shown in figure 11 are for an initial combustor pressure of 20 kPa, which corresponds to the experimental pressure in the reflected shock tunnel comparative combustion test (fig. 2). The results shown in figure 12 are for an initial combustor pressure of 101 kPa. The results of the simulations at 20 kPa clearly show that the presence of oxygen atoms in the test gas significantly increases the chemical energy yield. This increase is due primarily to an increase in the rate of the reaction

$$O + H_2 \rightarrow H + OH \tag{3}$$

which produces the highly reactive free radicals H and OH. The net result is an increase in the overall reaction rate. When the reactivity of the test gas atomic oxygen is controlled (simulations 3, 4, and 5 in fig. 11), the simulations produced essentially the same result, which indicates that very little of the test gas atomic oxygen is recombining to release dissociation energy. The primary mechanism for test gas oxygen atom consumption is reaction (3). The low atomic oxygen recombination rate is due to the low combustor pressure.

The effect of the combustor pressure on oxygen atom recombination is illustrated in figure 12 for an initial combustor pressure of 101 kPa. When the reactivity of the test gas oxygen atoms is altered, there is a significant effect on the pressure distribution and the chemical energy yield, which indicates recombination of the oxygen atoms is occurring and that dissociation energy is being released in the reaction zone. The predominant reaction enhancement, however, is still through reaction (3).

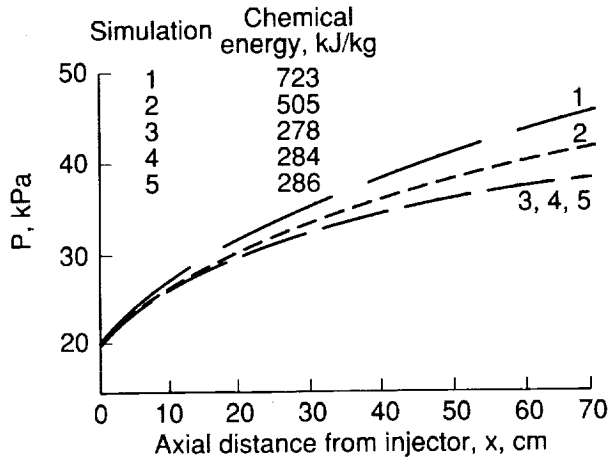

Figure 11. Results of parametric studies at an initial combustor pressure of 20 kPa.

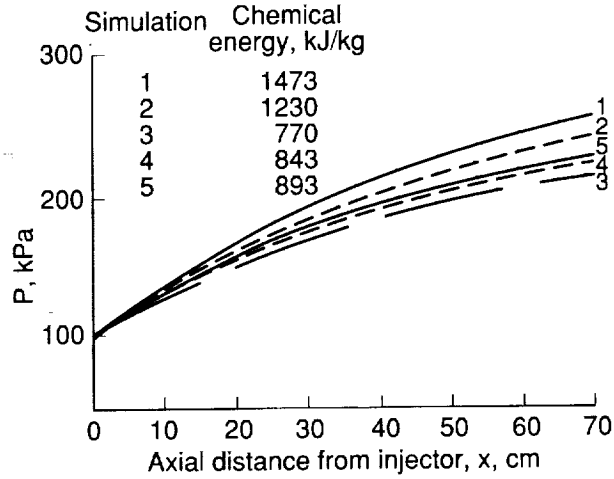

Figure 12. Results of parametric studies at an inital combustor pressure of 101 kPa.

The chemical kinetic analyses of the reflected shock tunnel experiments clearly indicate that combustion results can be affected by the presence of the dissociated oxygen. Although this effect on finite rate chemistry heat release can be modeled, and thus the combustion performance deduced from these experiments with dissociated test gas, other methods could produce the same chemical energy yield and pressure rise as expected in nondissociated air. Morgan et al. (ref. 2) suggest that the effect can be compensated by the appropriate reduction of the total oxygen content in the tunnel test gas. As noted previously, this approach is an attempt to reduce the chemical energy content of the test gas and correct for the oxygen atom heat of formation that is added to the heat release of the fuel. According to Morgan et al., the test gas mixture identified as reflected shock tunnel test gas *c* should simulate the expansion tunnel combustion results. Unfortunately, this mixture was not included in the comparative studies reported in reference 2. When this mixture was analyzed with the SCRAM3 code, the predicted pressure distribution was in very good agreement with the expansion tunnel combustion results.

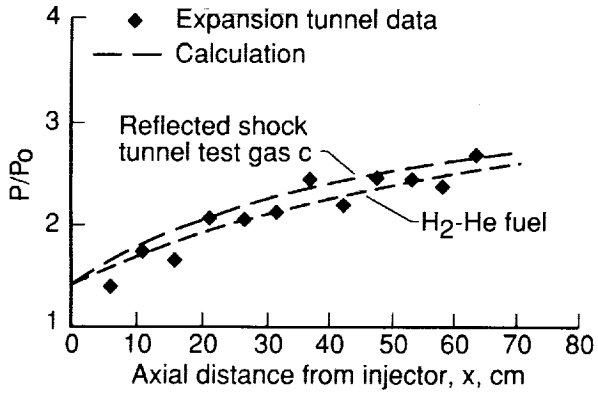

Figure 13. Calculated pressure distributions and expansion tunnel combustion data.

Another method that can be used to compensate for the effect of dissociated oxygen is to reduce the energy content of the injected fuel by adding an inert gas such as helium. The chemical energy released when a stoichiometric amount of hydrogen is reacted to equilibrium with the reflected shock tunnel dissociated air is about 2210 kJ/kg of reaction product, compared with 1860 kJ/kg for the expansion tunnel air. This difference is due to the release of some of the heat of formation carried by the dissociated oxygen. By diluting the fuel, it is possible to reduce the total energy release when the fuel reacts with the reflected shock tunnel air. For example, a fuel that consists of 45 percent H_2 and 55 percent He has an equilibrium chemical energy yield of 1855 kJ/kg when reacted with the reflected shock tunnel dissociated air. The pressure distribution predicted by the SCRAM3 combustor code when the fuel mixture is reacted with the reflected shock tunnel air is shown in comparison with the expansion tunnel combustion results in figure 13. Also shown in figure 13 is the predicted pressure distribution for the reflected shock tunnel air *c*. Each prediction is in good agreement with the experimental data, which suggests that either approach can be used. However, additional experiments are required to confirm these results.

Concluding Remarks

The purpose of this study was to investigate the effect of partially dissociated air on the combustion of hydrogen in high-speed flows. The study confirmed that the high concentration of dissociated oxygen present in reflected shock tunnel air at the Mach 17 test condition is responsible for the observed combustion enhancement. The presence of nitric oxide at the pressure levels of the present experiments does not affect the combustion process. The study also revealed that the combustion process is kinetically controlled in the experiments in both the expansion tunnel and the reflected shock tunnel. The chemical kinetic effect is the result of low combustion pressures and short residence times. The results of analytical studies suggest that the effect of partially dissociated air can be compensated either by altering the oxygen content of the reflected shock tunnel test gas or by reducing the hydrogen content of the fuel by dilution with an inert gas such as helium. Additional experimental studies, however, are needed to verify the proposed methods for controlling the effect of dissociated oxygen.

NASA Langley Research Center
Hampton, VA 23665-5225
May 14, 1992

References

1. Anderson, Griffin Y.; Kumar, Ajay; and Erdos, John I.: Progress in Hypersonic Combustion Technology With Computation and Experiment. AIAA-90-5254, Oct. 1990.

2. Morgan, R. G.; Bakos, R. J.; Tamagno, J.; Stalker, R. J.; and Erdos, J. I.: Scramjet Testing—Ground Facility Comparisons. Paper No. ISABE 91-194(L), Sept. 1991.

3. Bittker, David A.; and Scullin, Vincent J.: *General Chemical Kinetics Computer Program for Static and Flow Reactions, With Application to Combustion and Shock-Tube Kinetics.* NASA TN D-6586, 1972.

4. McLain, Allen G.; and Rao, C. S. R.: *A Hybrid Computer Program for Rapidly Solving Flowing or Static Chemical Kinetic Problems Involving Many Chemical Species.* NASA TM X-3403, 1976.

5. Rate Constant Committee, NASP High-Speed Propulsion Technology Team: *Hypersonic Combustion Kinetics.* NASP TM-1107, 1990.

6. Jachimowski, Casimir J.: *An Analytical Study of the Hydrogen-Air Reaction Mechanism With Application to Scramjet Combustion.* NASA TP-2791, 1988.

REPORT DOCUMENTATION PAGE

Form Approved
OMB No. 0704-0188

1. AGENCY USE ONLY *(Leave blank)*	2. REPORT DATE	3. REPORT TYPE AND DATES COVERED
	July 1992	Technical Paper

4. TITLE AND SUBTITLE
An Analysis of Combustion Studies in Shock Expansion Tunnels and Reflected Shock Tunnels

5. FUNDING NUMBERS
WU 505-62-40-04

6. AUTHOR(S)
Casimir J. Jachimowski

7. PERFORMING ORGANIZATION NAME(S) AND ADDRESS(ES)
NASA Langley Research Center
Hampton, VA 23665-5225

8. PERFORMING ORGANIZATION REPORT NUMBER
L-17025

9. SPONSORING/MONITORING AGENCY NAME(S) AND ADDRESS(ES)
National Aeronautics and Space Administration
Washington, DC 20546-0001

10. SPONSORING/MONITORING AGENCY REPORT NUMBER
NASA TP-3224

11. SUPPLEMENTARY NOTES

12a. DISTRIBUTION/AVAILABILITY STATEMENT
Unclassified Unlimited

Subject Categories 07, 25

12b. DISTRIBUTION CODE

13. ABSTRACT *(Maximum 200 words)*

The effect of initial nonequilibrium dissociated air constituents on the combustion of hydrogen in high-speed flows for a simulated Mach 17 flight condition was investigated by analyzing the results of comparative combustion experiments performed in a reflected shock tunnel test gas and in a shock expansion tunnel test gas. The results were analyzed and interpreted with a one-dimensional quasi-three-stream combustor code that includes finite rate combustion chemistry. The results of this study indicate that the combustion process is kinetically controlled in the experiments in both tunnels and that the presence of the nonequilibrium partially dissociated oxygen in the reflected shock tunnel enhances the combustion. Methods of compensating for the effect of dissociated oxygen are discussed.

14. SUBJECT TERMS
Supersonic combustion; Shock expansion tunnels; Reflected shock tunnel; Combustion modeling

15. NUMBER OF PAGES
10

16. PRICE CODE
A02

17. SECURITY CLASSIFICATION OF REPORT	18. SECURITY CLASSIFICATION OF THIS PAGE	19. SECURITY CLASSIFICATION OF ABSTRACT	20. LIMITATION OF ABSTRACT
Unclassified	Unclassified		